

# Iris Segmentation Techniques For Iris Diagnosis: a survey

Poovayar Priya M<sup>1</sup>, Ezhilarasan M<sup>2</sup>  
<sup>1</sup>Dept. of Computer Science and Engineering,  
E-mail ID: [poovayarpriya25@gmail.com](mailto:poovayarpriya25@gmail.com)

<sup>2</sup>Dept. of Information Technology PONDICHERRY ENGINEERING COLLEGE, Puducherry-605014  
E-mail ID: [mrezhil@pec.edu](mailto:mrezhil@pec.edu)

## Abstract:

The iris of the eye is the most complex tissue of the body. The iris is connected to the dura mater of the brain via 28,000 nerve endings that form part of the optic nerve (part of central nervous system). It is an extension of the brain, being incredibly endowed with hundreds of thousands of nerve endings, microscopic blood vessels, muscle and other tissues. The iris is connected to every organ and tissue of the body by way of the brain and nervous system. Nature has provided us with a miniature television screen showing the most remote portion of the body. In the recent years, due to the success of the deep learning models in the computer vision fields, there has been a large amount of works aimed at developing image segmentation approaches using deep learning model. In this survey, we provide a review on iris segmentation models covering the traditional models as well as recent deep learning methods. We examine the strengths and weaknesses of the various models and discuss promising future direction in this research area.

**Keywords:** Image processing, Image segmentation, deep learning, neural networks, Traditional methods, edge detection, iris diagnosis.

## I. INTRODUCTION

Image Segmentation is an important stage in the field of computer vision applications. Segmentation involves partitioning of the digital image into multiple objects [2]. Segmentation involves a wide range of applications of Content-based image retrieval, machine vision, medical imaging (locate tumors, measure tissue volumes, diagnosis, surgery planning, virtual surgery simulation, intra-surgery navigation), object detection (Pedestrian detection, face detection, brake light detection), Recognition tasks (face recognition, fingerprint recognition, iris recognition), Traffic control systems, video surveillance. Various range of algorithms includes Daugman method [2]-[5], Hough transform [8], Intensity based method [13], Thresholding based method [14], Pushing and pulling method [15], Ant colony optimization-based method [16], Edge detection method [17] for iris diagnosis.

Iris diagnosis or analysis useful method of assessment that offers the potential to expand the physician's understanding of a patient's overall state of health and vitality. Iris diagnosis offers a useful and quick screening method that may alert the physician to underlying problems as an aid to the holistic physician in nutritional counselling. In the eye, iris is the annulation part of some color that locates around the pupil. Mostly, iris is regarded as an inner organ of human body. However, it may be easily observed from exterior. Iris has a very fine structure that contains five layers of fibre like tissues. These tissues are very complex and reveal in various forms such as thread-like, linen-like, burlap-like, reticulation etc. The surface of iris contains also very complex texture structures such as crystals, thin threads, spots, concaves, radials, furrows, strips, etc.



Fig. 1. Segmentation of iris from eye image

Iris diagnosis studies the colored portion of the eye named iris. The iris is a highly innervated organ which is stimulated both by the external environment and as well as by the body. The structure of the iris mirrors the individual constitution; illnesses, harmful habits and aging can alter it. The iris analysis completes medical practice by supplying data on constitution, nervous response, damages caused by aging, illnesses and familiarity. Traditional methods have been applied for diagnosing iris which fails to give compromising results. Our survey covers the traditional methods for iris recognition, edge detection methods and deep learning methods which can be applied for iris diagnosis to get accurate results. We present a summary of the image segmentation models and provide a future direction for iris diagnosis based on deep learning methods.

## II. CLASSIFICATION OF IMAGE SEGMENTATION MODELS

- A. Traditional Methods
  - a) Daugman method

Daugman [2]-[5] presented a novel iris recognition system which forms the basis for most of the developmental activities in iris recognition till date. This method applied an integro-differential operator to detect the boundaries of limbic and pupil. The segmented iris is then converted into a rectangular form by applying polar transformation. Integro-differential Operator is used for detecting the circular shaped region of pupil and iris in captured image. Further he used to detect the arcs of lower and upper regions of eyelids [2]. Integro-differential operator is mathematically expressed as:

$$\text{Max}(r, x_0, y_0) \left| G_\sigma(r) * \left( \frac{\delta}{\delta r} \right) \int_{(r, x_0, y_0)} \frac{I(x, y)}{2\pi r} ds \right|$$

It continuously applies the operator on the captured image with the objective of getting a maximum contour integral derivative with continuously increasing radius at successively finer scales at the three parameters, i.e., centre coordinates (x0, y0) and radius (r). And also, Daugman [6] proposed a new segmentation algorithm which helps in handling off-axis iris images. Active contours have been used for segmentation. It is based on discrete Fourier series expansions of the contour data. By employing , Fourier components whose frequencies are integer multiples of 1/2p, closure, orthogonality and completeness are ensured. After that, segmentation of the iris from the eye using integro differential operator and normalized the iris created using Daugman’s method by Tapia et.al [7] and used the entire features from the normalized iris to classify gender. The annular region of the iris is transformed from cartesian coordinates to polar form. This results in a rectangular iris image. The size of the normalized iris can be determined by the radial resolution (r) and angular resolution (q) and can significantly influences the iris recognition rate. They used a normalized image of 20 (r) \* 240 (q).

b) *Hough Transform*

Wildes [8] applied the first derivative of the image intensity to find the location of edges corresponding to iris boundaries. Limbic and pupillary boundary are detected with the help of a gradient based binary edge map followed by circular Hough transform. This method explicitly models the upper and lower eyelids with parabolic arcs, whereas Daugman excludes the upper and lower portions of the image. This is one of the localization methods that is similar to daugman’s method, which is also based on the first derivative of the iris image intensity. The method implemented first discusses about obtaining an edge map of the iris by thresholding its magnitude of the iris intensity gradient:

$$|\nabla G(x, y) * I(x, y)|$$

$$\nabla \equiv \left( \frac{\partial}{\partial x}, \frac{\partial}{\partial y} \right) \text{ and}$$

$$G(x, y) = \frac{1}{2\pi\sigma^2} e^{-\frac{(x-x_0)^2 + (y-y_0)^2}{2\sigma^2}}$$

G(x,y) is a Gaussian smoothing function with scaling parameter σ selecting the proper scale of edge analysis. To maximize the defined Hough transform, the edge map is then used in a voting process to obtain a desired contour. The circle defined by the edge points corresponding at a maximum point in the Hough space with radius r and centre coordinates xc and yc according to the equation:

$$x_c^2 + y_c^2 - r^2 = 0$$

Ma et al. [9],[10] determined roughly the iris region in the eye image and then used canny edge detection and circular Hough transform to exactly compute the center and radius of the two circles in the determined region. Jaishanker et al. [11] designed a framework for cross sensor mismatch which used contour processing and circular Hough transform to detect the inner outer boundaries of the iris, respectively. Then the two ellipses are fitted to approximate the edges of the upper and lower eyelids. The iris region is then transformed using a polar structure and mapped to 20 \* 240 grid. Monro et al. [12] segmented an iris by a heuristic method based on the assumption that the rows and columns passing through the pupillary boundary will have larger gray-level variance than those not passing through the pupillary boundary. They assumed that the pupil is circular and because the boundary has a distinct edge feature, a circular Hough transform is used to find the center and radius of the iris. A horizontal line passing through the pupil center is scanned for the jumps in gray level on either side of the pupil to locate the outer boundary of the iris. The limbic boundary is normally circular but its center does not necessarily coincide with that of the pupil.

c) *Intensity based techniques*

Avila and Reillo [13] applied an intensity-based techniques for limbic and pupil boundary detection. The pupillary boundary used to initialize the active contour, which evolves to find the limbic boundary of the iris. First, the image of the eye is converted to gray scale and its histogram is linearly stretched, as to be able to take profit of all range given by the 256 levels of the gray scale. Then, following the ideas proposed by Daugmanin [2], a grid is placed over the image and testing each of the

points in the grid, the center of the iris, as well as the outer boundary; i.e., the border between the iris and the sclera, is detected making use of the circular structure of the latter. The detection is performed maximizing  $D$ , where

$$D = \sum_m \sum_{k=1}^5 (I_{n,m} - I_{n-k,m}),$$

$$I_{i,j} = I(x_0 + i \Delta r \cos(j \Delta \theta), y_0 + i \Delta r \sin(j \Delta \theta))$$

where  $(x_0, y_0)$  is a point in the grid taken as center, and  $I(x, y)$  is the gray level of the image at pixel  $(x, y)$ . This method of evolution from pupil to limbic iris boundary is computationally expensive.

d) *Thresholding based methods*

Vatsa et al. [14] applied a linear threshold on the eye image i.e. pixels with less intensity than the specified empirical value are converted to 0 (black) and pixels that are greater or equal to the threshold are assigned 1 (white). Freeman's chain code algorithm is used to find regions of 8-connected pixels having the value 0. This algorithm is applied to retrieve the black pupil of the image. From this region, the central moment is obtained. Starting from the center to both the extremities, boundaries are defined by the first pixel of intensity 1. The algorithm for finding the edges of the iris from eye image  $I(x, y)$  is as follows:

1. Center of pupil  $(Cpx, Cpy)$  and radius  $r$  are known using the pupil detection algorithm.
2. Apply Linear Contrast Filter on image  $I(x, y)$  to get the linear contrasted image  $P(x, y)$ .
3. Create vector  $A = \{a_1, a_2, \dots, a_w\}$  that holds pixel intensities of the imaginary row passing through the center of the pupil, with  $w$  being the width of the image  $P(x, y)$ .
4. Create vector  $R$  from the vector  $A$  which contains elements of  $A$  starting at the right fringe of the pupil and ending at the right most element of vector  $A$ . Similarly, another vector  $L$  is created which contains elements of  $A$  starting at the left fringe of the pupil and ending at the leftmost element of vector  $A$ .
5. For each side of the pupil (vector  $R$  for the right side and vector  $L$  for the left side):
  - a. Calculate the average window vector  $Avg = \{b_1, \dots, b_n\}$  where  $n = |L|$  or  $n = |R|$ . Vector  $Avg$  is subdivided into  $I$  windows of size  $z$ . The value of every element in the window is replaced by the mean value of that window.
  - b. Locate the edge point for both the vectors  $L$  and  $R$  as the first increment in value of  $Avg$  that exceeds a threshold  $t$ .

e) *Pushing and pulling method*

Zhenan Sun et al. [15] segmented the valid iris texture regions using pushing and pulling method from the original iris images. Since their focus is on iris image classification, they used this method for segmentation. Traditionally iris images are normalized into polar form. In their implemented, they got  $512 * 80$ -pixel size of normalized iris image. The flowchart for pushing and pulling method is shown in fig.2.

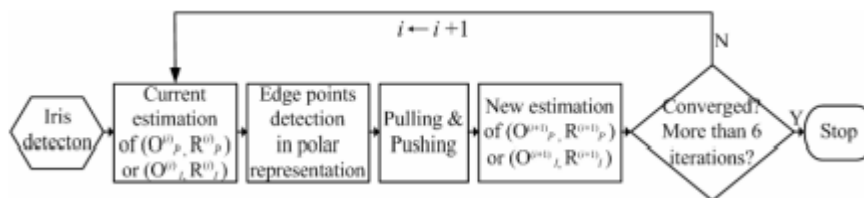


Fig.2. Pushing and pulling method

f) *Ant colony optimization*

Lin Ma et al. [16] focuses on studying the geometrical deformation in irises that are caused by gastrointestinal diseases, and measured the observable changes in the geometrical structures of irises that are associated with diameter, roundness and other geometric forms of the pupil and the collarette boundary. These boundaries are segmented through an ant colony optimization-based image segmentation algorithm (ACO-ISA). The algorithm for ACO is as follows:

- 1) Step-1: Initialize parameters consisting of  $\alpha, \beta, \gamma, \rho, k$  and  $A$ , and so on ; initialize pheromone distribution  $\theta(x,y)$ .
- 2) Step-2: For all ants, set up: find every ant agent arbitrarily at the territory array;
- 3) Step-3: For  $t=1$  to  $T_{max}$ , arrange: Step-4 to Step-12; Here  $T_{max}$  controls the maximum iterations.
- 4) Step-4: For all ants, arrange:
- 5) Step-5: calculate worldwide course chances  $P_i$ , in step with eqs. (3.1) and (3.4).
- 6) Step-6: pick the adjoining cell with the best  $P_i$ .
- 7) Step-7: If the selected cellular is stuffed by means of another ant, do: hold for the next ant.
- 8) Step-8: pass the ant.
- 9) Step-9: growth the pheromone at the mobile in step with eq. (3.2).
- 10) Step-10: keep for the following ant.
- 11) Step-11: Evaporate pheromone by using  $k$ , at all cells consistent with eq. (3.3).
- 12) Step-12: keep for the subsequent generation.
- 13) Step-13: give up.

### B. Edge Detection Methods

Boles and Boashash [17] proposed a circular edge detection in which the maximum diameter of the iris in the eye image is calculated. For comparing two images in order to calculate the diameter, one will be considered to be a reference image. The ratio of the maximum diameter of iris image to that of the reference image is also calculated. This ratio is used to make the virtual circles.

Pattabhi Ramaiah et al. [18] segmented an iris using canny edge detection followed by circular Hough transform. They normalized the iris using Daugman's rubbersheet model. In order to segment iris region, the segmentation parameters of the NIR (Near-infrared) iris image is applied on visible (Rchannel) iris image. The set of experiments were performed on iris images from 280 different classes which were properly segmented in visible and near-infrared channels.

Mamta Mittal [19] proposed a robust edge detection algorithm using multiple threshold approaches (B-Edge). The two fundamental limitations encountered are: edge connectivity and edge thickness. The proposed method successfully detects robust and thin edges with less noise. It provides with better edge continuity and also provides better entropy value. This proposal method does not work for blur images effectively. Computation of time needs to be improved. By implementing with deep learning approach, optimal results can be obtained.

Deepak Dhillon [20] presented an Enhanced Canny Edge Detection using Stochastic Resonance (SR) guided threshold maneuvering and window mapping which works as that of conventional Canny but produces better connected edges and reduces noise. The two main limitations are focused in this paper: Broken edges and noisy structures. A detailed analysis of CED along with SR is also presented. The proposed algorithm had a significant improvement over CED. But, non-inclusion of any pre/post processing has created some limitation in the performance of the algorithm. The future work focuses on addressing these limitations with designing deep neural network for better edge detection techniques.

### C. Deep Learning-Based Method

Yu Yongbin [21] proposed a network model named memristive network-based genetic algorithm (MNGA) by combining the memristive network and the genetic algorithm. MNGA based edge detection was proposed. To overcome the existing methods such as noise and difficult to design the individual's fitness and an edge information, this new edge detection methods consists of filtering technique and designed a fitness function to analyse every pixel. The algorithm involved in the GA based MN is as follows:

**Step 1** Initialize the MN and parameters of the GA, and the fitness of population can be calculated.

**Step 2** If the algorithm is not terminated,  $S_r(b)$ disposes individuals one by one. If not, go to Step 6.

**Step 3** After choosing two individuals  $b_1$  and  $b_2$  under the rule of  $S_r, C_r(b_1, b_2)$  is completed to obtain a new individual.

**Step 4** The process  $B_r(b)$ will be implemented to decide whether individuals are variable or not.

**Step 5** After processes  $S_r, C_r(b_1, b_2)$ , and  $B_r(b)$ , the new population is obtained. Then, the algorithm goes back to Step 2.

GA operator based on Memristive network:

$$FF(x,y) = \sum_{\substack{i=-1,0,1 \\ j=-1,0,1}} |P(x,y) - P(x+i,y+j)|$$

where  $P(x, y)$  denotes the  $x$ th row and  $y$ th column pixel value in the image.  $FF(x,y)$  denotes the fitness of pixel  $(x, y)$ . The performance is evaluated based on FoM which showed result as 62.7%.

Davood Karimi [22] proposed a different deep neural network based on self-attention between neighboring image patches and without any convolution operation which can achieve more accurate segmentation than FCNs. Traditional models which use convolution as their main building block, this model is based on self-attention between neighbouring 3D patches and achieved an accurate result. Starting with the input sequence of embedded and position encoded patches,  $X^0$  described above, the  $k$ <sup>th</sup> stage of the network performs the following operations to map  $X^k$  to  $X^{k+1}$ .

1)  $X^k$  goes through  $n_h$  independent heads in MSA. The  $i$ <sup>th</sup> head:

a) Computes the query, key, and value sequences from the input sequence using linear operations:

$$Q^{k,i} = E_Q^{k,i} \text{LN}(X^k), \quad K^{k,i} = E_K^{k,i} \text{LN}(X^k), \\ V^{k,i} = E_V^{k,i} \text{LN}(X^k)$$

where  $E_Q, E_K, E_V \in \mathbb{R}^{D_h \times D}$  and LN denotes layer normalization.

b) Computes the self-attention matrix and then the transformed values:

$$A^{k,i} = \text{Softmax}(Q^T K) / \sqrt{D_h} \\ \text{SA}^{k,i} = A^{k,i} V^{k,i}$$

2) Outputs of the  $n_h$  self-attention heads are stacked together and re-projected back onto  $\mathbb{R}^D$ :

$$\text{MSA}^k = E_{\text{reproj}}^k [\text{SA}^{k,0}; \dots; \text{SA}^{k,n_h}]^T$$

where  $E_{\text{reproj}} \in \mathbb{R}^{D \times D_h n_h}$

3) The output of the current multi-head self-attention module is computed using a residual operation:

$$X_{\text{MSA}}^k = \text{MSA}^k + X^k$$

4)  $X_{\text{MSA}}^k$  goes through a two-layer FFN to obtain the output of the  $k$ <sup>th</sup> stage of the network:

$$X^{k+1} = X_{\text{MSA}}^k + E_2^k \left( \text{ReLU} \left( E_1^k \text{LN}(X_{\text{MSA}}^k) + b_1^k \right) \right) + b_2^k$$

The proposed method evaluated based on DSC (Dice Similarity Coefficient) with 89.2% accuracy. The future work is, this model can be applied to other task in medical image analysis such as anomaly detection and classification.

Iman Aganj [23] presented the new atlas-based method for supervised soft segmentation of images, which produces the expected value of the label at each region of the new image instead of attempting to determine a single correct label. They computed the expected label value (ELV) map simply via a convolution with the key using fast Fourier transform (FFT). In case  $N$  atlases (affinely aligned in the same space) with manual labels are available, the equation can be written:

$$E := \frac{1}{N} \sum_{i=1}^N \mathbf{E}[L_i \circ T|I, J_i],$$

where  $J_i$  and  $L_i$  are the  $i$ <sup>th</sup> pair of atlas and manual-label images, respectively. The performance is evaluated based on DSC showed the result as 92%. Still the segmentation accuracy can be improved by using ELV map to augment the input to a CNN beyond the image itself.

Shumao Pang [24] proposed a novel two-stage framework named SpineParseNet to achieve automated spine parsing for volumetric MR images. The SpineParseNet consists of a 3D graph convolutional segmentation network (GCSN) for 3D coarse segmentation and a 2D residual U-Net (ResUNet) for 2D segmentation refinement. This two-stage segmentation framework reduces the memory costs during training and test phases. The primary advantage of the proposed method is GCN is employed to improve the discrimination of different spinal structures. The Semantic graph is generated as follows:

$$F^S = \sigma \left( A^e \sigma \left( A^e \sigma \left( A^e F^G W_1^e \right) W_2^e \right) W_3^e \right)$$

where  $W_1^e \in \mathbb{R}^{m \times m}$ ,  $W_2^e \in \mathbb{R}^{m \times m}$ , and  $W_3^e \in \mathbb{R}^{m \times m}$  are three trainable weight matrices.

As a result, SpineParseNet achieved accurate spine parsing for volumetric MR images. It achieved 0.87 with DSC as metric. But, the SpineParseNet fails to segment the top structure of the image. In the future, utilization of region-specific classifier can be used to segment the regions with high uncertainty to obtain better segmentation results.

Xiaomeng Li [25] presented a new semi-supervised method for medical image segmentation, where the network is optimized by a weighted combination of only labeled inputs for common supervised loss and of both labeled and unlabeled data for regularization loss. In semi-supervised segmentation, introduced a transformation-consistent strategy in the self-ensembling model to enhance the regularization effect for pixel-level predictions. The lack of labeled data motivates the study of methods which can be trained with limited supervision such as semisupervised learning. One limitation is that the assumption of both labeled and unlabeled data comes from the same distribution. But, in medical applications, labeled and unlabeled data may have different distributions with a domain shift. This method is general and can be widely used in other semisupervised medical imaging problems. In the future, an exploration of domain adaptation can be extended.

Xiaoting Han [26] presented a novel deep symmetric architecture of Unsupervised domain adaptation which consists of a segmentation sub-network and two symmetric source and target domain translation sub-networks. Existing UDA-based methods focus on minimizing the differences between distributions of source and target domains from the image translation or feature alignment. But, in this model a bidirectional alignment scheme over source and target translation sub-networks was proposed and also explored the semantic information from different style images. This method shows a significant advantages compared to the state-of-the-art methods. This method can be further improved to better generalize in the target domain.

Chenyu You [27] presented a Semi-supervised segmentation method named SimCVD, a simple contrastive distillation framework. Previous methods of semi-supervised learning face major challenges such as Suboptimal performance, geometric information loss and generalization ability. To address these problems: SimCVD is featured by: boundary-aware representations that incorporate rich information of the object shape, multi-task learning that jointly predicts a segmentation map along with a signed distance map and a pair-wise distillation objective. SimCVD obtained new state-of-the-art results. Further, the work can be extended to solve multi-class medical image segmentation tasks.

Yue Zhao [28] designed a two-stream graph convolutional network (TSGCN) model for segmenting a tooth. The state-of-the-art deep learning-based methods experiences different raw attributes reveal completely different geometric information i.e., the naïve concatenation of different raw attributes at the input phase brings unnecessary confusion in describing and differentiating between mesh cells. This TSGCN model can effectively handle inter-view confusion between different raw attributes to fuse their complementary information and learn discriminative multi-view geometric representations. Since this method is suited for only limited number of training samples, the future work can be extended to implement for large number of training samples. Kai Han [29] proposed a deep semi-supervised approach for liver CT image segmentation by integrating pseudo-labeling algorithm. The scale of training data remains to be the main bottleneck to obtain a deep segmentation model. A semi-supervised framework for liver image segmentation was introduced which generates high-quality pseudo labels for unlabeled images by utilizing the guidance from labeled images. The future work is to achieve more robust class representations formed by the network architecture and the number of output channel to better guide the generation of pseudo labels.

Cheng Ouyang [30] proposed a novel self-supervised few shot-segmentation framework for medical images named SSL-ALPNet. Conventional FSS methods are designed for segmenting images which relies on abundant annotated data of training class to learn image representations that generalize to unseen testing classes. But such a training is impractical in annotation scarce medical imaging scenarios. The proposed method exploits superpixel-based pseudo-labels to provide supervision signals. In addition to this, an effective adaptive local prototype pooling module was also proposed to boost segmentation accuracy. The proposed method is designed for one-way segmentation i.e., only one label class to be segmented at a time. The future work can be extended to multi-way segmentation where more than one classes are to be segmented.

Caiyong Wang [31] proposed a high efficiency deep learning based iris segmentation method named IrisParseNet. Since iris images are captured in non-cooperative environments often suffer from adverse noise which challenges many existing iris segmentation methods. To address this problem, the proposed approach gives a complete iris segmentation solution i.e., iris masking and parameterized inner and outer iris boundaries. The proposed method is compared with traditional iris segmentation methods on the newly annotated iris databases and shows a leading performance on various benchmarks. The future work can be extended to explore more efficient strategies to explicitly exploit the spatial relationship among iris mask, inner and outer iris boundaries to improve the segmentation performance.

Zhiyong Wang [32] trained a deep convolutional neural network (DCNN) that automatically extracts the iris and pupil pixels of each eye from input image. In this network, combination of UNet and SqueezeNet to train an efficient convolutional neural network for pixel classification. This system advances the state of the art in 3D eye gaze tracking using a single RGB camera. This approach performs good because it is fast, fully automatic and accurate. This system runs in real time on PCs and smart phones.

Ran Gu [33] makes use of multiple attentions in a CNN architecture and proposed a comprehensive attention-based CNN (CA-Net) for more accurate and explainable medical image segmentation. Paying an attention to the most relevant channels and scales is an effective way to improve the segmentation performance. CA-Net gives a comprehensive interpretation of how each spatial position, feature map channel and scale is used for prediction in segmentation tasks. The superiority of this network is that it achieves high explainability and efficiency than other methods. In the future, this method can be easily extended to segment 3D images as well.

**D. Other Methods**

Poursaberi and Araabi [34] proposed a method that is based on iris segmentation by using image morphological operators and applied suitable threshold. They performed the morphological operations (clean, spur and tilt) on binary image to remove the mentioned artifacts. Doyle et.al [35] segmented an iris using commercially available iris biometrics SDK (Software development kit) to extract the pupillary boundary and limbic boundary. The segmentation process divides each iris region into three parts: pupil, iris and sclera. The software outputs center point (x,y) and radius only. More accurate segmentation representation (ellipses, snakes) and mask (eyelids/eyelashes occlusion, spectral reflection) information are not available with this software.

Satish Rapaka et al. [36] applied GACs (Geodesic active contour) for segmented an iris which is associated with a novel stopping function. To evaluate the curves, the stopping function is used in GACs. To segment an iris, a contour is first initialized near the pupil, with a center (xp,yp) and radius rp. By applying a circular Hough transform to the binarized image, the center and radius of the initial contour are determined. To get faster segmentation results, an initial contour position is specified closer to the desired object boundaries. The contour is evolved then until stopping criterion is satisfied. This proposed method is robust for non-ideal iris and achieves a lower EER (Equal Error rate) of 0.6%.

Andrey kuehlkamp et al. [37] used OSIRIS (Open-source iris recognition software) (ver.4.1) to find out the center and radius of the iris from the eye. The software is mainly composed of four modules, namely segmentation, normalization, feature extraction and template matching. This paper uses segmentation and normalization from the software. For segmenting an iris region from the eye, segmentation approach used in OSIRIS 4.1 is contour edge detection and the normalization is done based on Daugman'srubbersheet model.

**Table 1.** Summary of the image segmentation models

S.no	Traditional methods	Deep learning methods	Other methods
1.	Integro-differential operator	MNGA based edge detection	OSIRIS
2.	Canny edge detection	Self-attention based neural network	Geodesic Active contours
3.	Contour processing and circular hough transform	Multi- Atlas Image Soft Segmentation	Iris biometrics SDK software
4.	Ant colony optimization based Image segmentation	SpineParseNet Segmentation framework	Morphological operators and thresholds
5.	Pushing and pulling method	Semi-supervised Image segmentation	Heuristic gray-level edge feature
6.	Active contours and generalized coordinates	Unsupervised Domain Adaptation	-
7.	Intensity based detection	SimCVD:Simple Contrastive Distillation Semi-supervised based segmentation	-
8.	Image intensity gradient and Hough transform	Two Stream Graph Convolution Network based Image Segmentation	-
9.	B-Edge connectivity algorithm.	A deep semi-supervised approach for liver image segmentation	-
10.	SR-guided Enhanced Canny Edge Detector	Self-supervised learning for few shot image segmentation	-
11.	-	Deep Multi-task Attention network for Iris Segmentation	-
12.	-	Deep Convolutional Neural network	-
13.	-	CA-Net: Comprehensive Attention Network	-

**III. CONCLUSION**

This paper discusses various image segmentation methods based on conventional methods, deep learning-based methods and many other methods. Deep learning-based methods have achieved impressive performance in various image segmentations tasks categorised into MNGA, Self-attention network, soft segmentation, SpineParseNet, Semi-Supervised and Unsupervised segmentation, SimCVD, GCN, DCN, CA-Net, among others. We summarized the various image segmentation models based on traditional methods, deep learning methods and other methods of image segmentation. The traditional method used for iris segmentation had some shortfall which can be overcome by deep learning methods. The performance of the various deep learning methods has been discussed. Based on this work, it is concluded that traditional methods fail to give accurate results, when applying deep learning-based segmentation method for iris diagnosis, it will give an accurate result which is our future direction in the field of iris diagnosis.

REFERENCES

- [1] Rafael C. Gonzalez, and Richard E. Wood, "Digital Image Processing", 3rd Edition, 2014.
- [2] J. G. Daugman, "Uncertainty relation for resolution in space, spatial frequency, and orientation optimized by two-dimensional visual cortical filters", *Journal of the Optical Society of America*, vol. 2, no. 7, pp. 1160 - 1169, Jul. 1985.
- [3] J. G. Daugman, "High confidence visual recognition of persons by a test of statistical independence", *IEEE transactions on pattern analysis and machine intelligence*, vol. 15, no. 11, pp. 1148 - 1161, Nov. 1993.
- [4] J. G. Daugman, "Biometric personal identification system based on iris analysis", U.S. Patent Number: 5 291 560, Mar. 1, 1994.
- [5] J. G. Daugman, "The importance of being random: Statistical principles of iris recognition", *Pattern Recognition*, vol. 36, no. 2, pp. 279 - 291, Feb. 2003.
- [6] J. Daugman, "New methods in iris recognition", *IEEE Transactions on Systems, Man, and Cybernetics, Part B (Cybernetics)*, vol. 37, no. 5, 2007.
- [7] Tapia, J.E. and Perez, C.A. "Gender Classification From NIR Images by Using Quadrature Encoding Filters of the Most Relevant Features", *IEEE Access*, vol. 7, pp. 29114-29127, Mar. 2019.
- [8] R. P. Wildes, "Iris recognition: An emerging biometric technology", *Proceedings of the IEEE*, vol. 85, no. 9, pp. 1348-1363, Sep. 1997.
- [9] L. Ma, T. Tan, Y. Wang, and D. Zhang, "Personal identification based on iris texture analysis", *IEEE transactions on pattern analysis and machine intelligence*, vol. 25, no. 12, pp. 1519-1533, Dec. 2003.
- [10] L. Ma, T. Tan, Y. Wang, and D. Zhang, "Efficient iris recognition by characterizing key local variations", *IEEE Transactions on image processing*, vol. 13, no. 6, pp. 739-750, Jun. 2004.
- [11] Pillai, J.K., Puertas, M. and Chellappa, R., "Cross-sensor iris recognition through kernel learning", *IEEE transactions on pattern analysis and machine intelligence*, vol. 36, no. 1, pp. 73-85, Jan. 2014.
- [12] D. M. Monro, S. Rakshit, and D. Zhang, "DCT-based iris recognition", *IEEE Transactions on Pattern Analysis Machine Intelligence*, vol. 29, no. 4, pp. 586-596, Apr. 2007.
- [13] C. Sanchez-Avila and R. Sanchez-Reillo, "Two different approaches for iris recognition using Gabor filters and multiscale zero-crossing representation", *Pattern Recognition*, vol. 38, no. 2, pp. 231-240, Feb. 2005.
- [14] M. Vatsa, R. Singh, and A. Noore, "Reducing the false rejection rate of iris recognition using textural and topological features", *Journal of Signal Processing*, vol. 2, no. 1, pp. 66-72, 2005.
- [15] Sun, Z., Zhang, H., Tan, T. and Wang, J., "Iris image classification based on hierarchical visual codebook", *IEEE Transactions on pattern analysis and machine intelligence*, vol. 36, no. 6, pp. 1120-1133, 2013.
- [16] Ma, L., Zhang, D., Li, N., Cai, Y., Zuo, W. and Wang, K., "Iris-based medical analysis by geometric deformation features", *IEEE journal of biomedical and health informatics*, vol. 17, no. 1, pp. 223-231, Jan. 2013.
- [17] W. W. Boles and B. Boashash, "A human identification technique using images of the iris and wavelet transform", *IEEE transactions on signal processing*, vol. 46, no. 4, pp. 1185- 1188, Apr. 1998.
- [18] Nalla, P.R. and Kumar, A., "Toward more accurate iris recognition using cross-spectral matching", *IEEE transactions on Image processing*, vol. 26, no. 1, pp. 208-221, Jan. 2017.
- [19] Mittal, M., Verma, A., Kaur, I., Kaur, B., Sharma, M., Goyal, L.M., Roy, S. and Kim, T.H., An efficient edge detection approach to provide better edge connectivity for image analysis. *IEEE access*, vol. 7, pp. 33240-33255, 2019.
- [20] Dhillon, D. and Chouhan, R., Enhanced Edge Detection Using SR-Guided Threshold Maneuvering and Window Mapping: Handling Broken Edges and Noisy Structures in Canny Edges. *IEEE Access*, vol. 10, pp. 11191-11205, 2022.
- [21] Yongbin, Y.U., Chenyu, Y.A.N.G., Quanxin, D.E.N.G., Tashi, N., Shouyi, L. and Chen, Z., Memristive network-based genetic algorithm and its application to image edge detection. *Journal of Systems Engineering and Electronics*, vol. 32, no. 5, 2021.
- [22] Karimi, D., Dou, H. and Gholipour, A., Medical Image Segmentation Using Transformer Networks. *IEEE Access*, vol. 10, pp. 29322-29332, 2022.
- [23] Aganj, I. and Fischl, B., Multi-Atlas Image Soft Segmentation via Computation of the Expected Label Value. *IEEE transactions on medical imaging*, vol. 40, no. 6, pp. 1702-1710, 2021.
- [24] Pang, S., Pang, C., Zhao, L., Chen, Y., Su, Z., Zhou, Y., Huang, M., Yang, W., Lu, H. and Feng, Q., SpineParseNet: Spine parsing for volumetric MR image by a two-stage segmentation framework with semantic image representation. *IEEE Transactions on Medical Imaging*, vol. 40, pp. 262-273, 2020.
- [25] Li, X., Yu, L., Chen, H., Fu, C.W., Xing, L. and Heng, P.A., Transformation-consistent self-ensembling model for semisupervised medical image segmentation. *IEEE Transactions on Neural Networks and Learning Systems*, vol. 32, no. 2, pp. 523-534, 2020.
- [26] Han, X., Qi, L., Yu, Q., Zhou, Z., Zheng, Y., Shi, Y. and Gao, Y., Deep symmetric adaptation network for cross-modality medical image segmentation. *IEEE transactions on medical imaging*, vol. 41, no. 1, pp. 121-132, 2021.
- [27] You, C., Zhou, Y., Zhao, R., Staib, L. and Duncan, J.S., Simcvd: Simple contrastive voxel-wise representation distillation for semi-supervised medical image segmentation. *IEEE Transactions on Medical Imaging*, 2022.
- [28] Zhao, Y., Zhang, L., Liu, Y., Meng, D., Cui, Z., Gao, C., Gao, X., Lian, C. and Shen, D., Two-Stream Graph Convolutional Network for Intra-Oral Scanner Image Segmentation. *IEEE Transactions on Medical Imaging*, vol. 41, no. 4, pp. 826-835, 2021.
- [29] Han, K., Liu, L., Song, Y., Liu, Y., Qiu, C., Tang, Y., Teng, Q. and Liu, Z., An Effective Semi-supervised Approach for Liver CT Image Segmentation. *IEEE Journal of Biomedical and Health Informatics*, 2022.
- [30] Ouyang, C., Biffi, C., Chen, C., Kart, T., Qiu, H. and Rueckert, D., Self-supervised Learning for Few-shot Medical Image Segmentation. *IEEE Transactions on Medical Imaging*, 2022.
- [31] Wang, C., Muhammad, J., Wang, Y., He, Z. and Sun, Z., Towards complete and accurate iris segmentation using deep multi-task attention network for non-cooperative iris recognition. *IEEE Transactions on information forensics & security*, vol. 15, pp. 2944-2959.
- [32] Wang, Z., Chai, J. and Xia, S., Realtime and accurate 3D eye gaze capture with DCNN-based iris and pupil segmentation. *IEEE transactions on visualization and computer graphics*, vol. 27, no. 1, pp. 190-203, 2019.
- [33] Gu, R., Wang, G., Song, T., Huang, R., Aertsen, M., Deprest, J., Ourselin, S., Vercauteren, T. and Zhang, S., CA-Net: Comprehensive attention convolutional neural networks for explainable medical image segmentation. *IEEE transactions on medical imaging*, vol. 40, no. 2, pp. 699-711, 2020.
- [34] A. Poursaberi and B. N. Araabi, "Iris recognition for partially occluded images: Methodology and sensitivity analysis", *EURASIP Journal on Applied Signal Processing*, vol. 2007, no. 1, pp. 20, Jan. 2007.
- [35] Doyle, J.S. and Bowyer, K.W., "Robust detection of textured contact lenses in iris recognition using BSIF", *IEEE Access*, vol. 3, pp. 1672-1683, 2015.
- [36] Rapaka, S. and Kumar, P.R., "Efficient approach for non-ideal iris segmentation using improved particle swarm optimisation-based multilevel thresholding and geodesic active contours", *IET Image Processing*, vol. 12, no. 10, pp. 1721-1729, Apr. 2018.
- [37] Kuehlikamp, A., Pinto, A., Rocha, A., Bowyer, K.W. and Czajka, A., "Ensemble of Multi-View Learning Classifiers for Cross-Domain Iris Presentation Attack Detection", *IEEE Transactions on Information Forensics and Security*, vol. 14, no. 6, pp. 1419-1431, Jun. 2019.